*Work supported in part by the U. S. Atomic Energy Commission.

[1]K. M. Watson, Phys. Rev. 15, 228 (1954).
[2]M. Kawaguchi and S. Minami, Progr. Theoret. Phys. (Kyoto) 12, 789 (1954).
[3]E. Fermi, Nuovo Cimento Suppl. 10, 17 (1955).
[4]C. Pellegrini and L. Tau, Nuovo Cimento 16, 973 (1960).
[5]R. H. Capps, Phys. Rev. Letters 2, 475 (1959).
[6]D. Branson, P. V. Landshoff, and J. C. Taylor, Phys. Rev. 132, 902 (1963).
[7]In this representation, a three-particle system in the center-of-mass frame is described by the total energy E, two energies E_i of any two particles, and the three Euler angles to specify the orientation of the triangle formed by E_1, E_2, and E_3. Then, going over to the angular momentum representation, one replaces the three Euler angles by J, M, Λ, where M is the projection of J on the space-fixed z axis, Λ its projection on the normal to the triangle $E_1E_2E_3$. Because of rotational invariance, the matrix elements do not depend on M. For details, see Ref. 6.
[8]R. L. Walker, California Institute of Technology Report No. CALT-68-158, 1968 (unpublished).
[9]R. G. Moorhouse and W. A. Rankin, Nucl. Phys. B23, 181 (1970).
[10]P. Bareyre, C. Bricman, and G. Villet, Phys. Rev. 165, 1730 (1968).
[11]C. H. Johnson, Jr., Lawrence Radiation Laboratory Report No. UCRL-17683, 1967 (unpublished).
[12]B. H. Bransden, P. J. O'Donnell, and R. G. Moorhouse, Phys. Rev. 139, B1566 (1965).
[13]A. Donnachie, R. G. Kirsopp, and C. Lovelace, Phys. Letters 26B, 161 (1968).
[14]L. D. Roper, R. M. Wright, and B. T. Feld, Phys. Rev. 138, B190 (1965).
[15]G. Giacomelli, P. Pini, and S. Stagni, CERN/HERA Report No. 69-1 (unpublished).
[16]We omit these and other details which can be found in the author's Ph.D. thesis, Department of Physics, University of Oregon, Eugene, Oregon, 1971.
[17]E. D. Bloom *et al.*, SLAC Report No. SLAC-PUB-653, 1969 (unpublished).

PHYSICAL REVIEW D VOLUME 6, NUMBER 3 1 AUGUST 1972

Final-State-Interaction Contributions to the Exotic Forward Peak in $\pi^- p \to K^+ Y^{*-}(1385)$ *

Dennis Sivers and Frank von Hippel
High Energy Physics Division, Argonne National Laboratory, Argonne, Illinois 60439
(Received 3 December 1972)

We calculate the contributions to the exotic exchange reaction $\pi^- p \to K^+ Y^{*-}(1385)$ in which the reaction $\pi^- p \to K^{*0}\Lambda$ feeds the $\pi^-\Lambda$ final-state interaction. The calculation contains no parameters. The final-state-interaction contribution can by itself account for the current data on the cross section and for the observed destructive interference between the K^{*0} and $Y^{*-}(1385)$ bands in the associated Dalitz plot in the final state $K^+\pi^-\Lambda$.

I. INTRODUCTION

Forward scattering in two-body and quasi-two-body meson-baryon reactions may usefully be categorized by the corresponding t-channel charge and hypercharge. When the exchanged quantum numbers are exotic, i.e., do not correspond to a possible quark-antiquark state, the absence of observed exotic meson resonances forces the phenomenologist to try to explain the process in terms of multiple nonexotic exchanges.

Many calculations have been made of exotic-exchange-reaction amplitudes.[1-3] They have all been multiple-scattering calculations in the sense that the exotic exchange is constructed from an iteration of amplitudes without exotic exchange connected by on-mass-shell two-body or quasi-two-body intermediate states. Because of uncertainties in the many nonexotic exchanged amplitudes involved, however, these calculations have been presented only as order-of-magnitude estimates of the differential cross sections and of the energy dependence.

When one of the final particles in an exotic-exchange reaction is unstable, we have the possibility that the last particle exchanged in the reaction is on its mass shell. An example of such a process occurs in the reaction

$$\pi^- p \to K^+ Y^{*-}(1385) \to K^+(\Lambda\pi^-). \tag{1.1}$$

One multiple-exchange contribution to this reaction comes about when the nonexotic exchange reaction

$$\pi^- p \to K^{*0}\Lambda$$

is followed by a second nonexotic exchange reaction

$$K^{*0}\Lambda \to K^+ Y^{*-}(1385)$$

in which a physical pion is exchanged. Such a process in which a physical particle is exchanged in the final step is traditionally called a "final-state-interaction" process. Final-state-interaction contributions have not previously been calculated in treatments of exotic exchange processes.

In this paper we examine, as an example, the final-state contributions to (1.1). We obtain a cross section which is the same order of magnitude as that which is observed for exotic exchange processes such as

$$\pi^- p \to K^+ \Sigma^-,$$

in which final-state-interaction effects do not contribute. It appears, therefore, that final-state-interaction effects must be taken into account in any serious treatment of exotic exchange processes going to quasi-two-body final states. We find, furthermore, that the final-state-interaction contribution gives rise to some distinctive interference phenomena[4] between the K^{*0} and $Y^{*-}(1385)$ bands in the final state of the reaction

$$\pi^- p \to K^+ \pi^- \Lambda \tag{1.2}$$

when the final K^+ is restricted to be going forward. Effects of this kind and of the predicted size are observed in the data[5-7] for reaction (1.2).

In the final-state-interaction approach, we begin with a model of the "bare" amplitude for the reaction (1.2) which does not incorporate the effects of the final-state $\pi\Lambda$ interaction. When the K^+ is produced forward, it is assumed that the bare amplitude is identical to the physical amplitude except that the $Y^{*-}(1385)$ Breit-Wigner term is absent. For intermediate energies the Dalitz plot for reaction (1.2) is dominated by the $K^*(890)$ and $K^*(1420)$ resonance bands, both of which overlap the position of the Y^{*-}.

Physically, the fact that the K^* and Y^* bands overlap means that a π^- from a K^* decay can have a c.m. energy in the $\pi\Lambda$ system appropriate to the Y^*. When the $\pi\Lambda$ pair is in a relative $J^P = \frac{3}{2}^+$ angular momentum state, they will, therefore, undergo resonant scattering. The scattering will, of course, preserve the energy in the $\pi\Lambda$ c.m. frame, but the direction of the π and, hence, the πK subenergy can change. The result is that, at the position of the $Y^{*-}(1385)$, the final-state interaction scatters events out of the K^* regions into the remainder of the Y^* band with *no change in the total number of events in this interval of* $\pi\Lambda$ *mass.*

We examine the currently available data[5-7] on reaction (1.2) for evidence of the final-state-interaction mechanism. At 4.5 GeV/c, *no significant* $Y^{*-}(1385)$ *peak is observed until the contributions of the* K^* *bands* are removed. (See Fig. 1, taken from Ref. 7.) Within the admittedly severe limitations of the statistics, it appears that the K^* and Y^* bands interfere destructively in such a way that there are holes in the K^* bands which compensate for the events in the Y^* mass peak seen outside of the overlap regions. This is a distinctive prediction of the final-state-interaction model. Since we find that the predicted magnitude of the interference effect appears to be in accord with experiment, we suggest further testing and refinement of this approach as improved data become available, as well as applications to other quasi-two-body processes where it may be appropriate.

The contribution to exotic exchange amplitudes considered in this model may prove to have an analogous role to the one-pion-exchange contribution to some nonexotic exchange amplitudes – a useful reference point for attempts at more comprehensive calculations. In fact, from one point of view, we are looking at one-pion exchange in a new setting. In the approximation of K^* dominance of the Dalitz plot before rescattering, our final-state-interaction model is mathematically equivalent to a component of a multiple-scattering model in which reaction (1.1) proceeds dominantly as a result of two successive nonexotic-exchange forward-scattering amplitudes:

$$\pi^- p \to K_n^{*0} \Lambda, \tag{1.3}$$

$$K_n^{*0} \Lambda \to K^+ Y^{*-}(1385), \tag{1.4}$$

where $n = 1, 2$ refer respectively to the $K^*(890)$ and the $K^*(1420)$. It may be (as crude estimates sug-

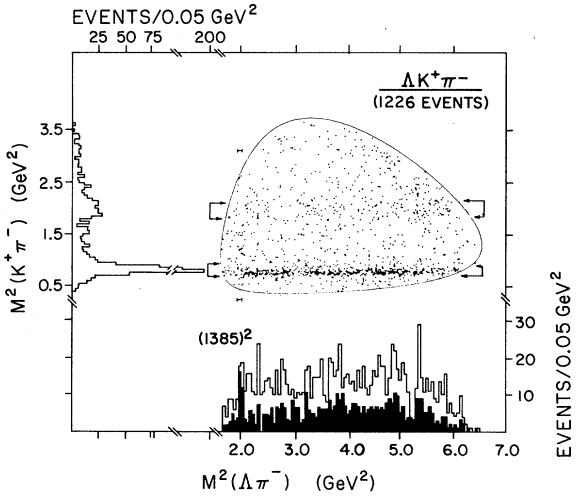

FIG. 1. The Dalitz plot of $\pi^- p \to K^+ \pi^- \Lambda$ at beam momentum 4.5 GeV/c, taken from Crennell *et al.*, Ref. 7. Also shown are the projections on $s_K = \pi^- K^+$ (GeV^2) and $s_\Lambda = \pi^- \Lambda$ (GeV^2). The shaded portion of the s_Λ projection consists of those events not in the K^* bands.

gest) that this sequence dominates other possible contributions to (1.1), with the result that the data display the interference characteristics of a final-state interaction because the amplitude for reaction (1.4) contains a strong "exchanged" pion pole in the physical region. The pole residue may, of course, be calculated from the experimental K^* and Y^* decay widths, and if we keep only the on-mass-shell part of this pole term, we recover the final-state-interaction model. In our detailed presentation, we show explicitly that our results are not sensitive to unknown phases and helicity structure of reactions (1.3) since, because of the small mass of the pion, these complications approximately factor out.

In Sec. II we will review the experimental data on reaction (1.1) and the relationship of our model to the previous model calculations which have been made. In Sec. III we will present a systematic development of the final-state-interaction calculation and compare its predictions with the data at 4.5 GeV/c. Our results are presented so that the predictions of the model at other energies may easily be calculated as the data become available. In Sec. IV we detail an argument based on duality whose results are used in Sec. III to fix the relative phase of the two K^* production amplitudes. The relationship between our calculation and the general topic of dual models is also discussed. Finally, in Sec. V, we present our conclusions.

II. EXOTIC EXCHANGE: THE EXPERIMENTAL SITUATION AND THEORETICAL OUTLOOK

Figure 2 shows the angular distribution of reaction (1.1) at the various energies at which it has been studied.[5-7] At high energy, we see that the exotic forward peak dominates the allowed backward peak associated with baryon exchange. Figure 3 shows the energy-dependence reaction (1.1) and, for comparison, that of the forward differential cross section for the reaction[1,7]

$$\pi^- p \to K^+ \Sigma^-, \tag{2.1}$$

which has no final-state-interaction contributions of the type considered here.

As we see, information on reaction (1.1) is severely limited because of its small cross section. As is the case with all exotic-exchange reactions, efforts to study the t-channel exchange mechanism must make compromises between ensuring that the energy is high enough so that the asymptotic mechanism is dominant and having the energy low enough so that the number of events allows statistically significant inferences to be made. The data which currently best meet these twin criteria for reaction (1.1) are the 1226-event sample on reaction (1.2) from a $\pi^- p$ bubble-chamber exposure at a beam momentum of 4.5 GeV/c, $s = 9.3$ GeV^2.[7] The Dalitz plot for this final state is shown in Fig. 1. For most of our discussion, we will concentrate on an explanation of the distribution of those events in this Dalitz plot associated with a forward K^+.

The main feature of Fig. 1 is the presence of two prominent K^* resonance bands, the $K^*(890)$

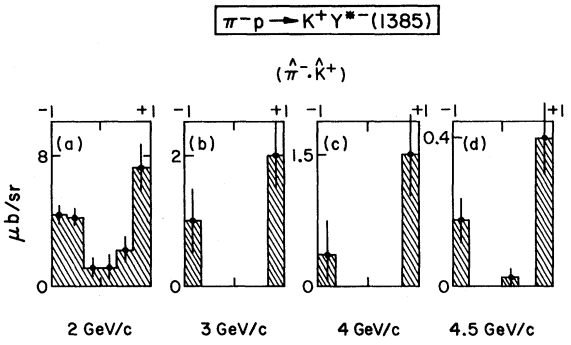

FIG. 2. The angular distribution for $\pi^- p \to K^+ Y^{*-}$ at the beam momenta 2, 3, 4, and 4.5 GeV/c. Already, at intermediate energy, we see the exotic forward peak dominates the allowed backward peak. (Taken from Ref. 7).

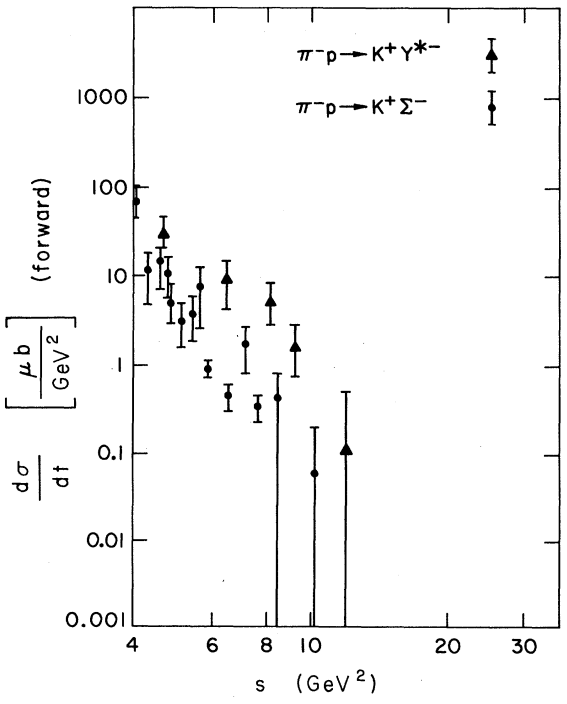

FIG. 3. The energy dependence of the forward peak in $\pi^- p \to K^+ Y^{*-}$ compared with that of $\pi^- p \to K^+ \Sigma^-$. (Data on $\pi^- p \to K^+ \Sigma^-$ taken from summary in Ref. 1).

and the $K^*(1420)$, containing approximately $\frac{3}{4}$ of the total number of events. At this energy, both K^* bands overlap the position of the $Y^{*-}(1385)$, and we will exploit this fact in our discussion below. This limits the range of lab energies at which our derivation is valid to the range at which this overlap takes place, an interval in beam momentum from 3.8 to 8.5 GeV/c. We discuss how to apply some of the same physical ideas at energies outside this range in Sec. III, but the confrontation with experiment becomes less direct. Within the range of energies where the overlap takes place, our calculation is very straightforward and involves no arbitrary parameters.

The calculation described in this paper falls within the general approach in which exotic exchange occurs as a result of multiple nonexotic exchanges. Other calculations of exotic exchange have been presented, based on Feynman diagrams[3] or the Reggeized absorption model.[1,2]

All these calculations are mathematically similar to the calculation we describe here with one important difference. They have been designed for reactions with two stable particles in the final state, such as (2.1). Our approach, on the other hand, has been specifically constructed to deal with resonances in three-body final states.

We believe that certain features of the exotic exchange mechanism become more transparent when we consider more than two particles in the final state and that studying exotic exchange in these situations can, therefore, be very interesting.

Extracting quasi-two-body reactions from data on three-particle final states for the purpose of studying exotic exchange has been thought ambiguous because kinematic reflections can cause certain broad mass enhancements.[8] These data do not suffer from that defect. The Dalitz plot of Fig. 1 shows no evidence for any sort of kinematic enhancement. In the region excluding the K^* bands, the background under the narrow Y^* signal is, within statistics, quite flat.[7] However, it may be of interest that the final-state-interaction effect can be calculated in the presence of a sizable kinematic reflection, as we shall show later.

III. THE FINAL-STATE-INTERACTION PRESCRIPTION FOR $\pi^- p \to K^+ Y^{*-}(1385)$

In this section we present our final-state-interaction calculation and discuss its physical implications.

The calculation. The diagram corresponding to the final-state-interaction model for reaction (1.2) is shown in Fig. 4(a). In this diagram, all straight lines represent the momenta of physical, on-mass-shell particles.[9] The two terms inside the brackets represent the disconnected and connected parts of the $\pi^-\Lambda$ S matrix. To the extent that this S matrix satisfies elastic two-body unitarity, we are guaranteed that the final-state-interaction prescription will conserve the total number of events in a given region of $\pi^-\Lambda$ mass.

The amplitude external to the brackets is, in this formulation, treated as a source of the π^- flux onto

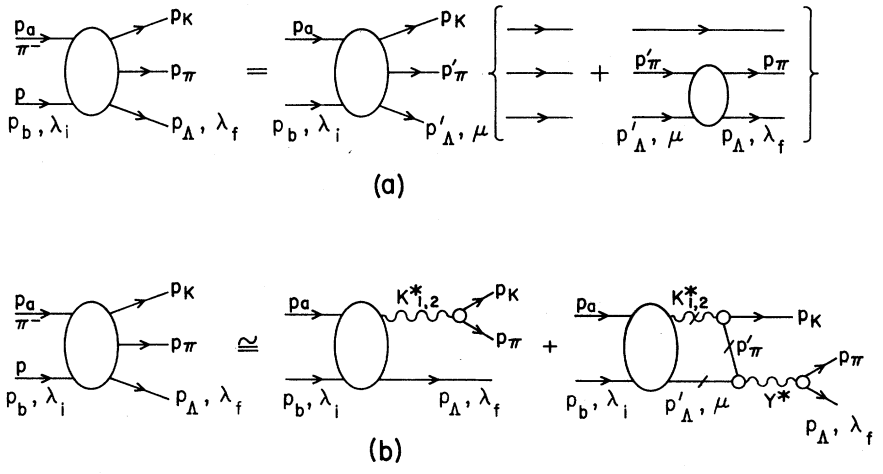

FIG. 4. (a) Diagramatic representation of the final-state-interaction model for $\pi^- p \to K^+ \pi^- \Lambda$. When the K^+ is forward in the c.m. frame, the full amplitude is represented by a "bare" amplitude without the Y^* Breit-Wigner term in the $\pi\Lambda$ subenergy postmultiplied by the $\pi\Lambda$ scattering matrix. In the approximation that we go to the Y^* pole in the $\pi\Lambda$ connected part and assume that the "bare" amplitude is dominated by K^* production, we obtain the double-scattering description shown in (b). In the rescattering contribution, the K^*'s, Λ, and π^- are all on their mass shells.

the Λ which the final-state-interaction rescatters from the original direction.[4, 10, 11] The separation implied by Fig. 4(a) is useful only to the extent that we can, in some way, determine this first term, i.e., the form of the amplitude in the absence of a final-state interaction. In this section we will make the assumption that the first term contains no exchange in the exotic $t_{\pi K}$ channel and, therefore, when the K^+ is produced forward, no $Y^*(1385)$ pole in the $\pi^-\Lambda$ channel. When we compare our model with the data of Ref. 7, we will discuss the evidence for this assumption.

The equation corresponding to Fig. 4(a) is

$$M_{\lambda_f\lambda_i}(s, s_K, s_\Lambda, \theta_K, \varphi_K, \varphi) = M^{(1)}_{\lambda_f\lambda_i}(s, s_K, s_\Lambda, \theta_K, \varphi_K, \varphi) + \sum_\mu \left(\frac{i}{8\pi^2}\right) \int d\Omega' \left(\frac{q_\pi M_\Lambda}{(s_\Lambda)^{1/2}}\right) M^{\pi\Lambda}_{\lambda_f\mu}(s_\Lambda, \theta, \varphi; \theta', \varphi') \times M^{(1)}_{\mu\lambda_i}(s, s'_K, s_\Lambda, \theta_K, \varphi_K, \varphi') . \tag{3.1}$$

Here λ_i, μ, and λ_f are helicity indices for the initial, intermediate, and final states; $s_K \equiv (p_\pi + p_K)^2$ and $s_\Lambda \equiv (p_\pi + p_\Lambda)^2$ are the Dalitz-plot invariants, and q_π is the magnitude of the pion three-momentum in the $\pi\Lambda$ c.m. frame. The angles θ_K and φ_K refer to K^+ production in the over-all c.m. frame and θ and φ are the π^- angles in the $\pi\Lambda$ helicity frame. Primed symbols refer to the intermediate state when the variables they represent have values different from those in the final state.

Figure 4(b) indicates symbolically the approximations we now make to Eq. (3.1).

(1) We approximate the amplitude $M^{\pi\Lambda}$ by a $J^P = \frac{3}{2}^+$ Breit-Wigner function at the position of the $Y^*(1385)$. In the limit that the Λ momentum in the $\pi\Lambda$ c.m. frame is small compared to its value in the over-all c.m. frame, its helicity structure can be approximated by

$$M^{\pi\Lambda}_{\lambda_f\mu} \cong \frac{4\pi M_Y}{q_\pi M_\Lambda} \left(\frac{b_{\pi\Lambda}}{x_Y - i}\right) \{2\hat{q}_\pi \cdot \hat{q}'_\pi \delta_{\lambda_f\mu} + i[\vec{\sigma} \cdot (\hat{q}_\pi \times \hat{q}'_\pi)]_{\lambda_f\mu}\} , \tag{3.2}$$

where the σ's are the Pauli matrices, $x_Y \equiv (M_Y{}^2 - s_\Lambda)/M_Y\Gamma_Y$, and $b_{\pi\Lambda} \cong 0.9$ is the $\pi\Lambda$ branching fraction of the $Y^*(1385)$. The directions of the unit three-vectors $\hat{q}_\pi$ and $\hat{q}'_\pi$ in Eq. (3.2) are shown in Fig. 5.

(2) To do the integration over $\cos\theta'$ in (3.1), we use the relation

$$s'_K = M_\pi{}^2 + M_K{}^2 + 2E_\pi E_K + 2q_\pi q_K \cos\theta' \tag{3.3}$$

(where the energies and momenta are evaluated in the $\pi\Lambda$ c.m. frame) and take advantage of the fact that the Dalitz plot, Fig. 1, indicates that the dependence of the amplitude $M^{(1)}$ on s_K will be dominated by the $K^*(890)$ and $K^*(1420)$ Breit-Wigner terms. We therefore approximate $M^{(1)}$ by

$$M^{(1)}_{\lambda_f\lambda_i}(s, s_K, s_\Lambda, \theta_K, \varphi_K, \varphi) \cong \sum_{\substack{n=1,2 \\ \lambda_n}} 4\pi \left(\frac{4b_n}{3q_n\Gamma_n}\right)^{1/2} M^n_{\lambda_f\lambda_n\lambda_i}(s, \theta^*_n) e^{i(\lambda_f - \lambda_n - \lambda_i)\varphi^*_n} Y^{\lambda_n}_n(\omega_n, 0)/(x_n - i) . \tag{3.4}$$

Here $n = 1, 2$ refers to the $K^*(890)$ and the $K^*(1420)$, respectively. θ^*_n, φ^*_n, and λ_n are the K^*_n production angles and helicity; b_n is the πK branching fraction, while $x_n \equiv (m_n{}^2 - s_K)/m_n\Gamma_n$. The angle ω_n which appears in the spherical harmonic is the K^+ angle in the K^*_n helicity frame and is related to s_Λ by

$$s_\Lambda = m_\pi{}^2 + M_\Lambda{}^2 + 2E^{(n)}_\pi E^{(n)}_\Lambda + 2q^{(n)}_\pi q^{(n)}_\Lambda \cos\omega_n . \tag{3.5}$$

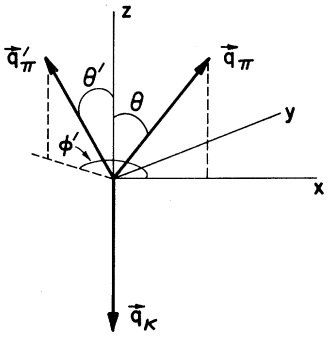

FIG. 5. Directions of the intermediate ($\vec{q}'_\pi$) and final ($\vec{q}_\pi$) pion momenta in the $\pi\Lambda$ frame. The K^+ momentum is along the negative z axis, and the x axis is chosen so that the final pion momentum has azimuthal angle equal to zero.

(3) The contribution of the Breit-Wigner terms in (3.4) to the integral over $\cos\theta'$ can be divided into two parts. In the narrow-resonance limit, only the imaginary parts contribute, giving the "on-mass-shell" term which, for our purposes, can be approximated by a δ function in $\cos\theta'$. The real part contributes a term to the principal-value portion of the integral which will be small when, at the position of the Y^*, the K^* resonance band is a few half-widths away from the Dalitz-plot boundary. Requiring both the K^* resonances to be well within the physical region limits the range of beam momentum in which our procedure is

valid without modification from 3.8 to 8.5 GeV/c.

(4) In order to do the integration over φ' in (3.1), we note that in the over-all c.m. system, when $s_\Lambda \cong M_Y^2$, varying φ' corresponds to rotating the intermediate K^* direction around the final K^+ direction on a cone whose opening angle is very small because of the small pion mass. The value of the cosine of this opening angle as a function of s is shown in Fig. 6. The effect of the φ' integration, then, is to "smear" $\cos\theta^*$ and φ^* in a small region around $\cos\theta_K$ and φ_K, respectively. Neglecting this smearing allows us to factor out the K^* production amplitudes so that the result of the integrations in (3.1) becomes particularly simple.

Choosing the x axis in the $\pi\Lambda$ helicity system so that $\varphi = 0$, we get

$$M_{\lambda_f\lambda_i}(s, s_K, s_\Lambda, \theta_K, \varphi_K) = \sum_{n,\lambda_n,\mu} 4\pi\left(\frac{4b_{\pi\Lambda}}{3q_n\Gamma_n}\right)^{1/2}\left(\frac{\delta_{\lambda_f\mu}}{(x_n - i)} - \frac{d_n}{(x_Y - i)}[2\cos\theta\,\delta_{\lambda_f\mu} - i\sigma^y_{\lambda_f\mu}\sin\theta]\right)$$

$$\times M^n_{\mu\lambda_n\lambda_i}(s, \theta_K)\, e^{i(\lambda_f - \lambda_n - \lambda_i)\varphi_K} Y_n^{\lambda_n}(\omega, 0)\,. \tag{3.6}$$

In this equation

$$d_n \equiv \frac{\pi m_n \Gamma_n \cos\theta_n\, b_{\pi\Lambda}}{2q_\pi q_K}\,, \tag{3.7}$$

where $\cos\theta_n$ is obtained from (3.3) by setting $s_K = m_n^2$. Values of the d_n are given as functions of s in Fig. 7. The d_n fall off asymptotically as $1/s$, but it is obvious from Fig. 7 that we are not in the asymptotic region at $s = 9.3$ GeV^2. Equations (3.6) and (3.7) are the main results of the final-state-interaction model for this reaction. We will compare their predictions directly with data later in this section. At this point, however, it is instructive to take an illustrative digression into the physics of the calculation.

The constraint of probability conservation. To understand more directly how the values of d_n have been fixed by the unitarity of the $\pi\Lambda$ S matrix, consider, as a simple example, a situation where we can neglect the contribution of the $K^*(1420)$ term in (3.6). Squaring the $n = 1$ term, summing over final Λ helicities, averaging over initial helicities, and imposing parity conservation the differential cross section is found to be proportional to

$$d\sigma \propto \sum_{\lambda_i\lambda_f\lambda} |M^{(1)}_{\lambda_i\lambda\lambda_f}|^2\, |\, Y_1^\lambda(\omega, 0)|^2 \left(\frac{1}{x_1^2 + 1} + \frac{(d_1)^2(1 + 3\cos^2\theta)}{x_Y^2 + 1} - \frac{4d_1\cos\theta(x_Y x_1 + 1)}{(x_1^2 + 1)(x_Y^2 + 1)}\right)\,. \tag{3.8}$$

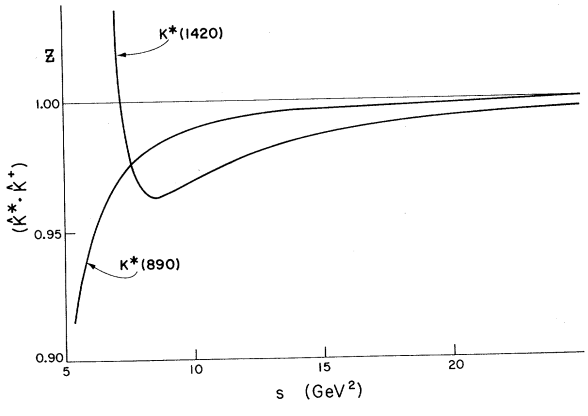

FIG. 6. Cosine of the angle in the over-all c.m. frame between the K^+ and the $K^*(890)$ and between the K^+ and $K^*(1420)$.

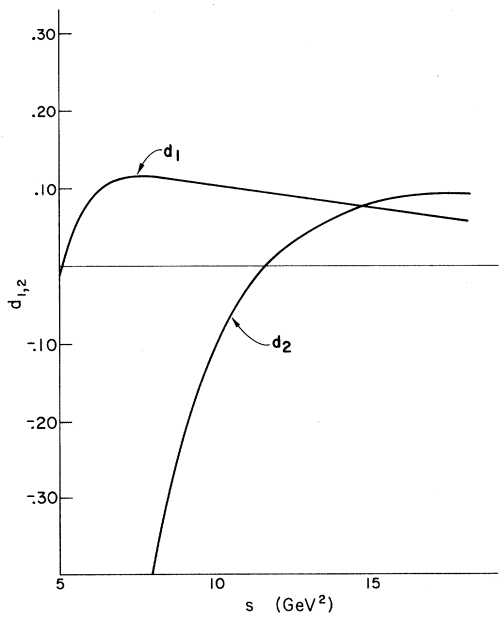

FIG. 7. Values of d_1 and d_2 given by Eq. (3.7) as a function of s.

We can now see that the terms in the brackets which depend on d_1 serve to rescatter events from inside the K^* resonance band to outside it. Taking $x_Y = 0$ in (3.8) and using the relation

$$x_1 = \frac{2q_\pi q_K}{m_1\Gamma_1}(\cos\theta_1 - \cos\theta), \tag{3.9}$$

where $\cos\theta_1$ is the value of $\cos\theta$ in (3.3) when $s_K = m_1^2$, the condition that the number of events be the same as in the absence of rescattering is

$$\int_{-1}^{+1} d(\cos\theta)\left(d_1^2(1+3\cos^2\theta) - \frac{4d_1\cos\theta}{(2q_\pi q_K/m_1\Gamma_1)^2(\cos\theta_1-\cos\theta)^2+1}\right) = 0. \tag{3.10}$$

Again, in the narrow-resonance limit, when $\cos\theta_1$ is displaced from the boundary, it is a good approximation to replace the second term in the integral by a δ function. The nontrivial solution to (3.10) is then given by

$$d_1 = \frac{\pi m_1\Gamma_1\cos\theta_1}{2q_\pi q_K}, \tag{3.11}$$

which is just the same as the result (3.7) except that we have neglected the inelasticity of the Y^* resonance and set $b_{\pi\Lambda} \cong 1$.

What has happened here is that the interference term between the K^* and Y^* Breit-Wigner terms is negative and causes a dip in the K^* band which just compensates in projection for the events scattered into the rest of the Y^* band. This qualitative prediction of the model seems to be realized in the data. Notice in the Dalitz plot of Fig. 1 that there is some indication of the destructive interference predicted by (3.6) at the intersection of the K^* bands with the Y^* and that there is no significant Y^* enhancement in the projection of the total Dalitz plot.

The relative phase and coherence of the K^* production amplitude. In order to apply our model to the data, we have to have some recipe for the coherence and relative phase of the two K^* production amplitudes in (3.6). If the K^* production mechanism involves K exchange, the contributions will be coherent and the relative phase of the $K^*(890)$ and $K^*(1420)$ Breit-Wigner terms in (3.6) at the intersection with the Y^* should be essentially the same as in backward $\pi^- K^+$ elastic scattering where they are of opposite sign by virtue of their opposite parities. In Sec. IV we will give arguments based on duality to show that this can be expected to be true also for the K^* exchange contribution to the production amplitudes. Note that since d_1 and d_2 are of opposite sign at $s = 9.3$ GeV^2 (see Fig. 7), this is precisely the phase that maximizes the number of events scattered out of the K^* bands at this energy. Using (3.6) and (3.7) at the energy of Crennel *et al.*,[7] we predict a depletion factor for the K^* bands of about 0.58, due to the final-state interaction. (At s near 11.5 GeV^2, d_2 goes through zero and changes sign, and its contribution begins to interfere destructively with the term proportional to d_1.)

Confronting the Dalitz plot. The final problem in comparing the model with data is to determine the population of the K^* bands in the absence of any final-state interaction. Since the Y^* band intersects the K^*'s near the edge of the Dalitz plot, an extrapolation of the K^*-band population in this region is subject to end-effect uncertainties. However, our assumption that there was no Y^* enhancement associated with forward K^+ in the total $\pi\Lambda$ mass distribution and the property of the final-state interaction that it conserves the number of events in a given region of $\pi\Lambda$ mass allows us to circumvent this extrapolation. The procedure is as follows:

(1) After selecting events with forward K^+, we determine the shape of the total $\pi\Lambda$ mass distribution in the region of the Y^*.

(2) We fit the $\pi\Lambda$ mass distribution for events outside the K^* bands on either side of the Y^* and thus obtain an estimate for the background under Y^*.

(3) All events above background are assumed to have been originally in one of the K^* bands. In this way, we obtain the s_Λ projection of the K^* events in the absence of a final-state interaction.

(4) The final-state interaction results in a Breit-Wigner-shaped hole in the projection of the K^* bands at the position of the $Y^{*-}(1385)$ whose depth is, for the data of Crennell *et al.*,[7] greater than one half (0.58) of the weight of the original projection.

(5) These events appear outside the K^* bands since the total probability is conserved.

The comparison of our predicted interference effect with the data of Crennell *et al.*[7] is shown in Figs. 8 and 9.

Away from the intersection with the K^* bands, the model predicts that the Y^* events are distributed according to the $\lambda_{Y^*} = \pm\frac{1}{2}$, $(1+3\cos^2\theta)$ rule. Within statistics, this prediction is consistent with the data.

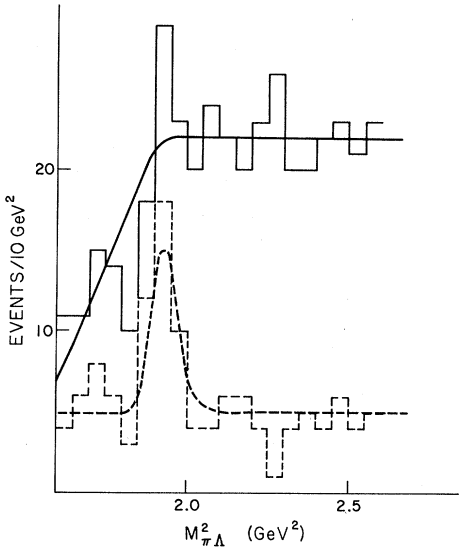

FIG. 8. The solid histogram is the projection of the Dalitz plot at 4.5 GeV/c on s_Λ with a cut to ensure forward K^+. The solid curve is a hand-drawn fit. The dashed histogram has K^* events removed, and the dashed curve is the prediction of the final-state-interaction model. (Data by private communication with the authors of Ref. 7.)

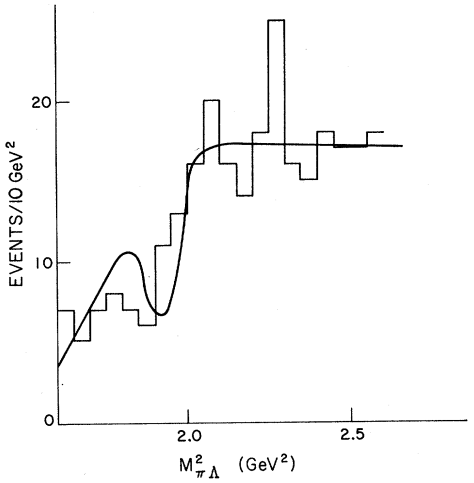

FIG. 9. Projection of the events in the K^* bands. The curve is the prediction of our model.

The discussion so far has not considered the possibility of a kinematic reflection of the kind discussed by Berger.[8] Although no significant reflection is present in this data, it is interesting to consider how our results would be modified if such an effect were present. First, any broad kinematic effect present in the region between the K^* bands should be included in the background as discussed above. It would be quite easy to separate this broad enhancement from the narrow Y^* signal. Second, a kinematic enhancement inside the K^* bands due to nonisotropic distribution of the decay pions in the K^* rest frame would, after the final-state interaction, cause proportionally more events to be in the Y^* Breit-Wigner term outside the K^* bands.

Other exotic exchange contributions. Within statistics, our final-state-interaction prescription accounts for all the Y^* signal associated with forward K^+, but the statistics are so limited that we really have not tested the accuracy of our approximation that this is the only contribution to exotic exchange in the $t_{\pi K}$ channel. If, with better data, any Y^* signal in the *total* $\pi\Lambda$ mass distribution is found at small $t_{\pi K}$, it must be attributed to another mechanism for exotic exchange. In fact, such other contributions, although not quantitatively calculable, are present and (judging from calculations of such contributions to the exotic exchange reaction $\pi^- p \to K^+ \Sigma^-$) can be expected to be of the same order of the final-state-interaction contribution which we have calculated here. Our model considers only a particular component of a multiple-scattering Regge cut. In the J plane associated with $t_{\pi K}$, the amplitude for $\pi^- p \to K^+ Y^{*-}$ described by (3.1) contains a finite Regge cut for every Regge-pole contribution to reaction (1.3) with length depending on the interval of "smearing" due to the integration over φ'. The approximation of neglecting the smearing leading to (3.6) and (3.7) can be thought of as an effective pole approximation to the finite cut. In the general absorption prescription,[1-3] other intermediate states and "off-mass-shell" pion exchange both contribute other segments to an infinite Regge cut. These other contributions are, in general, out of phase with the $\pi^- p \to K^* \Lambda$ amplitude and contribute to a total Y^* enhancement.

Unphysical pion exchange. If we believe in the general validity of the absorption approach and are interested in the problems associated with taking the exchanged pion in Fig. 4(b) off the mass shell, then we can consider continuing (3.6) and (3.7) to a region where no overlap between the $K^*(890)$ and the $Y^*(1385)$ occurs. Since we are then dealing with off-mass-shell pions, unitarity no longer holds, i.e., the condition (3.10) no longer holds and a total enhancement could occur at the position of the Y^*. In the continuation of (3.6) to this region, we could think of events moving in from outside the physical Dalitz plot by "rescattering" an unphysical pion onto its mass shell and producing a total Y^* enhancement. Looking at the various ways of making this continuation in terms of Fig. 4(b), we can connect with the various models for multiple exchange in which the final exchange is a

pion. Reggeizing the pion and inserting a form for the Regge residue function will give one sort of continuation, a form-factor approach requiring certain smoothness properties will give another. A related aspect is the continuation of the $\pi^-\Lambda$ S matrix in (3.1) to the Σ^- pole in order to calculate a contribution to $\pi^-p \to K^+\Sigma^-$. Any assumption concerning the methods of these continuations produces an ambiguity not present in (3.6) when the resonance bands overlap. This is why absorption-model-type calculations of other contributions to exotic exchange amplitudes are less reliable than those which we have calculated.

IV. DUALITY AND THE FINAL-STATE-INTERACTION PRESCRIPTION

The calculation presented in Sec. III connects quite naturally with the three-component view of duality espoused by Veneziano.[12] In this interpretation of dual models, exotic exchange in the absence of narrow exotic resonances is a consequence of corrections made to a narrow-resonance amplitude in order to make it consistent with unitarity. Our approach to $\pi^-p \to K^+Y^{*-}$ would therefore be equivalent to this type of correction if we inserted a dual, narrow-resonance model for the amplitude $M^{(1)}$ into Eq. (3.1).

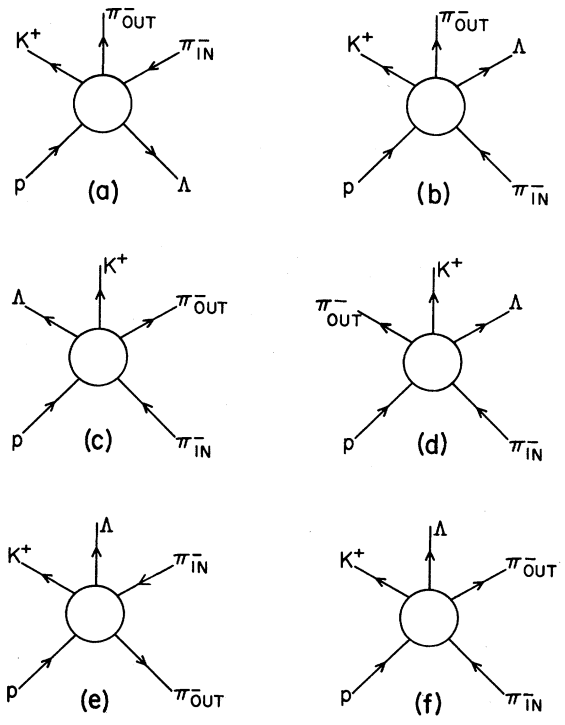

FIG. 10. Diagrams illustrating the singularity structure of a dual model without exotic resonances for $\pi^-p \to K^+\pi^-\Lambda$. Poles appear in channels defined by two adjacent particles.

To see this connection, consider the singularity structure of a dual model for $\pi^-p \to K^+\pi^-\Lambda$. This is in the complex of reactions related by crossing discussed by Hoyer, Petersson, and Törnqvist.[13] The singularity structure is defined by the diagrams shown in Fig. 10. Each diagram in this figure represents an ordering of the external particles such that the channels defined by two adjacent particles are nonexotic and have poles. In a narrow-resonance model, when we eliminate amplitudes with poles in exotic channels we eliminate any form of exotic exchange whatsoever. The naive form of "unitarization" usually used for B_5 phenomenology, which consists of giving the trajectory functions in the argument of the B_5 arbitrary imaginary parts, does not remedy this situation. It merely inserts thresholdlike singularities in channels which already have resonances without adding any singularities to exotic channels. Exchanges in exotic channels have to be present after any reasonable unitarization procedure, and the final-state-interaction prescription discussed in Sec. III, when applied to a dual model for $M^{(1)}$, is part of a larger scheme of absorptive corrections treated in Ref. 12.

One of the reasons for connecting the final-state-interaction approach to duality in this way is that the assumption made about the relative phase of the K^* production amplitudes in Sec. III can be obtained by considering a form for the "bare" amplitude $M^{(1)}$ based on a dual model.

For small $t_{\pi K}$ in the strict absence of any exotic resonances, a narrow-resonance model for $\pi^-p \to K^+\pi^-\Lambda$ must satisfy a superconvergence sum rule in s_K. If this sum rule is obeyed semilocally, in the manner commonly described as Dolen-Horn-Schmid duality,[14] the relative sign of the $K^*(890)$ and the $K^*(1420)$ Breit-Wigner terms in (3.6) must be negative in each helicity amplitude so that their contributions to the sum rule approximately cancel. This relative phase is a quite general feature of any narrow resonance amplitude with no exotics in the π^-K^- channel and does not depend crucially on a particular formulation of the amplitude in terms of B_5 functions.[15]

A specific dual model for the "bare" amplitude. One thing a specific dual model can give is the energy dependence of the forward peak in $\pi^-p \to K^+Y^{*-}$. In the method described in Sec. III, we would have to have, at each energy, the complete Dalitz plot for $\pi^-p \to K^+\pi^-\Lambda$ (with the K^+ restricted to be forward) in order to calculate the final-state-interaction contribution using (3.6) and (3.7). If we have a phenomenological B_5 model for $M^{(1)}$, we can

easily obtain the necessary information. Within the framework of the Harari-Rosner[16] (HR) quark-diagram rules, a B_5 amplitude for (1.2) should be constructed:

$$M^{(1)}_{\mathrm{HR}} \propto [\alpha_1 B_5(c) + \beta_1 (B_5(d) + B_5(e)) + \gamma_1 B_5(f)] . \tag{4.1}$$

An alternate choice, allowing diagrams with nonplanar quark lines, is favored by Hoyer, Petersson, and Törnqvist[13] (HPT):

$$M^{(1)}_{\mathrm{HPT}} \propto [\alpha_2 B_5(a) + \beta_2 B_5(b) + \gamma_2 B_5(c)] . \tag{4.2}$$

In the kinematic region we are considering (large s, small $t_{p\Lambda}$, and small $t_{\pi K}$) only diagrams (c) and (a) of Fig. 10 remain significant, and the two alternatives become distinguishable only by the signature of the exchange in the $\bar{p}\Lambda$ channel. This makes no difference for our applications, and we do not attempt to decide between the two alternatives here.[17] The singularity structure of the amplitude in this limit is indicated in Fig. 11. It can be seen that the amplitude has the K^* pole in s_K which, in Sec. III, we assumed was the dominant feature of the nonexotic amplitude.

We can now also explicitly see the prediction of the B_5 model for the relative phases of the K^* Breit-Wigner terms in (3.6) on the basis of the dominance of diagrams (b) and (c) of Fig. 10. In the limit shown in Eq. (4.2), a specific expansion of the B_5 amplitude in terms of K^* poles corresponding to (3.4) is

$$M^{(1)}_{B_5} \to K\, {}_2F_1(\cdots) s^{\alpha_{K^*}(t_{\bar{p}\Lambda})} \left(\alpha_2 + \gamma_2 e^{-i\pi\alpha_{K^*}(t_{\bar{p}\Lambda})}\right) \times B_4(1 - \alpha_{K^*}(s_{\pi K}), 1 - \alpha_\rho(t_{\pi\pi})) , \tag{4.3}$$

where α_{K^*} and α_ρ are the K^* and ρ Regge trajectories, and α_2 and γ_2 are as in (4.2). For $s_{\pi\Lambda}$ $M_Y{}^2$ and $s = 9$ GeV^2, the kinematic factor K and the hypergeometric function ${}_2F_1(\cdots)$ are slowly varying as we change $s_{\pi K}$, ranging from 1.00 at $m_1{}^2$ to 1.06 at $m_2{}^2$. The relative sign of the K^* and K^{**} pole residues can then be found by expanding the B_4 function in (4.3):

$$B_4(1 - \alpha_{K^*}(s_{\pi K}), 1 - \alpha_\rho(t_{\pi\pi})) = \frac{1}{\alpha'}\left(\frac{1}{s_{\pi K} - m_1{}^2} + \frac{\alpha_\rho(t_{\pi\pi})}{s_{\pi K} - m_2{}^2} + \cdots\right) . \tag{4.4}$$

The sign of $\alpha_\rho(t_{\pi\pi})$ can easily seem to be negative for $t_{\pi K}$ and $t_{p\Lambda}$ fixed and small $t_{\pi\pi}$,

$$t_{\pi\pi} = -s_{\pi K} + 2m_\pi{}^2 + m_K{}^2 - t_{\pi K} + t_{\bar{p}\Lambda} . \tag{4.5}$$

This relative minus sign between the two Breit-Wigner terms is a well-established general feature of duality and has to do with the fact that in backward $\pi^- K^+ \to \pi^- K^{*+}$ the resonance contributions to a finite-energy sum rule (FESR) must cancel on the average. We therefore feel justified in taking this sign as known in our calculations in Sec. III.

Using a complete B_5 model for $M^{(1)}$ based on (4.1) and (4.3) and the B_5 Monte Carlo program of Berger,[17] the energy dependence of the final-state-interaction prescription was calculated by one of us (DS). The results were found to be almost independent of whether the Harari-Rosner or the Hoyer-Petersson-Törnqvist formulation was used and are shown in Fig. 12.

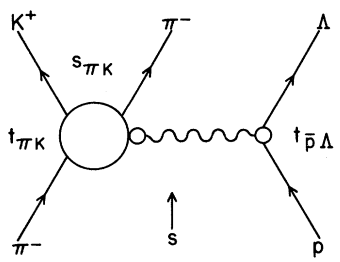

FIG. 11. Kinematics of K^* production amplitudes.

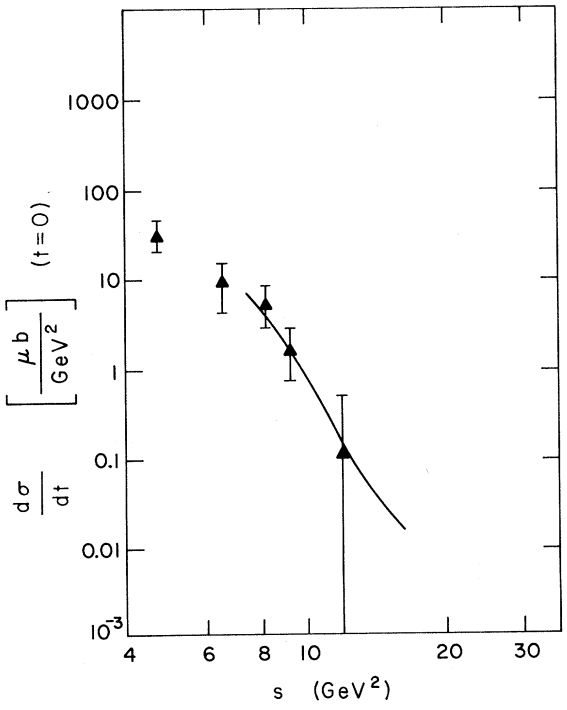

FIG. 12. Energy dependence for forward peak in $\pi^- p \to K^+ Y^{*-}$ predicted assuming a phenomenological B_5 model for the "bare" amplitude for $\pi^- p \to K^+ \pi^- \Lambda$ and incorporating a final-state $\pi^-\Lambda$ interaction.

Lovelace has described an elegant, unified treatment of Regge cuts in the context of the dual field-theory model.[18] Lovelace's approach, if successful, could raise the level of our understanding of exotic exchange far beyond that of the calculation presented here.

V. CONCLUSIONS

The idea of a final-state interaction has been around in particle physics for a long time. It will continue to be useful whenever it is feasible in some way to separate a source of particles from their subsequent scattering. If it is indeed possible to neglect exotic exchange in the "bare" amplitude for $\pi^- p \to K^+ \pi^- \Lambda$, we probably have a situation in which making this separation is as close to the textbook ideal as can be possible in dealing with systems of strongly interacting particles.

The general feature of our calculation, interference of resonance bands resulting in no total enhancement in the projection of the Dalitz plot, appears to have some likelihood of being correct experimentally. It should be tested thoroughly because the calculation of the magnitude of the interference is quite definite and involves no parameters so that, if experimental refinements prove its predictions invalid, then the applicability of the final-state-interaction approach to strongly interacting systems becomes extremely questionable. Similar reactions, such as $\pi^+ n \to \pi^- \pi^+ p$, with overlapping resonance bands where physical pions can be "exchanged" ought to be examined as well. In some respects, even more information about interference effects can be obtained when resonance bands are broad.

If experimental evidence substantiates the validity of the final-state-interaction approach to exotic exchange, studying situations in which resonance bands cease to overlap so that physical particle exchange continues into off-mass-shell exchange becomes an exciting possibility.

VI. ACKNOWLEDGMENTS

We would like to thank R. Arnold and E. Berger for several stimulating and informative discussions. We are grateful to D. Rust for bringing our attention to the problem and to Kwan-Wu Lai for providing us with a Dalitz plot from his experiment (Ref. 7) containing the data used in Figs. 8 and 9. We also thank J. D. Jackson for bringing the work of C. Schmid (Ref. 4) to our attention.

---

*Work performed under the auspices of the U. S. Atomic Energy Commission.

[1]C. Quigg, Nucl. Phys. B34, 77 (1971).

[2]R. J. Rivers, Nuovo Cimento 57A, 174 (1968); C. B. Chiu and J. Finkelstein, *ibid.* 59A, 92 (1969); C. Michael, Phys. Letters 29B, 230 (1969); F. S. Henyey, G. L. Kane, and J. J. G. Scanio, Phys. Rev. Letters 27, 350 (1971); N. Dean, Nucl. Phys. B7, 311 (1968); A. B. Kaudalov and B. Karnakov, Yad. Fiz. 11, 216 (1970) [Sov. J. Nucl. Phys. 11, 121 (1970)].

[3]C. P. Singh and B. K. Agarwal, Phys. Rev. 177, 2350 (1969); 182, 1910 (1969); Phys. Rev. D 1, 363 (1970); Lett. Nuovo Cimento 1, 756 (1969); 2, 605(E) (1969).

[4]C. Schmid, Phys. Rev. 154, 1364 (1967).

[5]P. M. Dauber, P. Hoch, R. J. Manning, D. M. Siegal, M. A. Abolins, and G. A. Smith, Phys. Letters 29B, 609 (1969).

[6]M. A. Abolins, O. I. Dahl, J. Danburg, D. Danes, P. Hoch, D. H. Miller, R. Rader, and J. Kirz, Phys. Rev. Letters 22, 427 (1969).

[7]D. J. Crennell, H. A. Gordon, K. W. Lai, J. Louie, J. M. Scarr, and W. H. Sims, Phys. Rev. Letters 26, 1280 (1971).

[8]E. L. Berger, Phys. Rev. Letters 23, 1139 (1969).

[9]We emphasize this to distinguish the approach from, for example, the Feynman-diagram calculations of Ref. 3. We have not included on the diagrams indications of the appropriate continuations in the momentum variables since, to the approximations which we work, these are irrelevant. For example, the one-pion exchange in Fig. 4(b) is real in the s channel.

[10]J. D. Jackson, Nuovo Cimento 25, 1038 (1962).

[11]I. J. R. Aitchison, Nuovo Cimento 35, 434 (1964).

[12]G. Veneziano, in *Proceedings of the International Conference on Duality and Symmetry in Hadron Physics*, Tel Aviv, 1971 (Weizmann Science Press of Israel, Jerusalem, 1971).

[13]B. Petersson and N. A. Törnqvist, Nucl. Phys. B13, 629 (1969); N. A. Törnqvist, *ibid.* B18, 530 (1970); P. Hoyer, B. Petersson, and N. A. Törnqvist, *ibid.* B22, 497 (1970).

[14]R. D. Dolen, D. Horn, and C. Schmid, Phys. Rev. 166, 1768 (1968).

[15]For a discussion see, e.g., D. Sivers and J. Yellin, Rev. Mod. Phys. 43, 125 (1971).

[16]H. Harari, Phys. Rev. Letters 22, 562 (1969); J. L. Rosner, *ibid.* 22, 689 (1969).

[17]The review of E. L. Berger [in *Phenomenology in Particle Physics, 1971,* edited by C. Chiu, G. Fox, and A. Hey (Caltech, Pasadena, 1971)] contains a comprehensive discussion of this problem.

[18]C. Lovelace, Phys. Letters 34B, 500 (1971).